Supplementary Information

Construction of Mn-N-C nanoparticles with multienzyme-like properties and photothermal performance for effectively treating bacterial infections

Yong Ding,[a] Xiao-Chan Yang,[a] Ya-Ya Yu,[a] Sheng-Nan Song,[a] Bo Li,[a] Xue-Yao Pang,[a] Jian-Jian Cai,[b] Chun-Huan Zhang,[b] Shan Huang,[a,c] Ya-Mu Xia*[a], Wei-Wei Gao*[a]

[a] *State Key Laboratory Base of Eco-chemical Engineering, College of Chemical Engineering, Qingdao University of Science and Technology, Qingdao 266042, China*

[b] *Township Central Clinic of Masanzi, Binzhou 251907, China*

[c] *The Third Affiliated Hospital of Xuzhou Medical University, Xuzhou 221000, China*

* Corresponding Address:

gww501@qust.edu.cn (W.-W. Gao); xiayamu@126.com (Y.-M. Xia)

1. Chemicals and reagents

$Zn(NO_3)\cdot 6H_2O$, hydrogen peroxide (30%), 5,5′-dithiobis(2-nitrobenzoic acid) (DTNB), *N,N*-dimethylformamide (DMF), and *o*-phenylenediamine were purchased from Sinopharm Chemical Reagent Co. Ltd. 2-Methylimidazole, poly(ethylene glycol) (PEG_{2000}), 3-propyl-2-[5-(3-propyl-2(3H)-benzothiazolylidene)-1,3-pentadien-1-yl]-iodide(1:1) [diSC3(5)], and crystal violet (CV) were obtained from Aladdin Reagent (Shanghai, China). 3,3′5,5′-tetramethylbenzidine (TMB), *o*-phenylenediamine, 5,5-dimethyl-1-pyrroline-*N*-oxide (DMPO) and glutathione (GSH) were obtained from Sigma-Aldrich. All other chemicals were reagent grade or better. All reagents and solvents were used as received. The deionized water of resistivity 18.2 MΩ cm^{-1} was used in all experiments. MRSA and AREC were provided by Sichuan Provincial People's Hospital, Chengdu, China.

2. Apparatus

Scanning electron microscopy (SEM) images were obtained on a JEOL JSM-6700F at a working voltage of 15 kV after platinum coating for 90 s. Transmission electron microscopy (TEM), energy dispersive X-ray spectroscopy (EDS) and EDS element mapping were acquired on the Talos F200X (integrated with Super-X EDS). XPS (X-ray photoelectron spectrometry, AXIS SUPRA) and XRD (X-ray diffraction, ULTIMALV) were employed to evaluate the phase composition of the samples on a X-ray diffractometer (Cu K_α radiation, $k = 0.15406$ nm). UV-vis absorbance measurements were carried out on a PEERSEE TU-1810 UV-vis spectrophotometer. The ζ-potential and size of the Mn-N-C NPs was

measured in a Zetasizer 3000HS analyzer. All electron spin resonance (ESR) measurements were carried out on a JEOL JES FA200 spectrometer at ambient temperature. Wound temperature changes in mice during treatment were photographed using an infrared thermography camera (TOPLIA TMi 120S).

3. Calculation of the photothermal conversion efficiency (η) of Mn-N-C NPs

Mn-N-C NPs aqueous solutions with different concentrations (0–200 μg mL^{-1}) were exposed to an 808 nm laser irradiation (1.0 W cm^{-2}) for 600 s, and the temperature was recorded every 30 s by a thermocouple probe. Mn-N-C NPs aqueous dispersion (0.2 mL) with different concentrations (0, 25, 50, 100, and 200 μg mL^{-1}) were exposed to an 808 nm laser irradiation (1.0 W cm^{-2}) for 600 s, then shutted off the laser for cooling the solution to room temperature. Heating and cooling temperature patterns of 20 μg mL^{-1} Mn-N-C NPs were recorded. The η of Mn-N-C NPs was calculated according to the following equations:

$$\eta = [hS(T_{max}-T_{surr})-Q_{diss}]/I(1-10^{-A808}) \quad \text{(S1)}$$

$$\tau_s = mC_p/hS \quad \text{(S2)}$$

Where h is the heat-transfer coefficient, S is the surface area of the container, T_{max} is the equilibrium temperature, T_{surr} is the ambient temperature, Q_{diss} is the heat obtained by container under 808 nm laser irradiation, I is the density of laser power, A_{808} is the absorbance of the Mn-N-C NPs suspension at 808 nm, and τ_s is the time constant obtained from Figure S2.

4. Peroxidase-like catalytic activity

The peroxidase (POD)-like catalytic assays of materials were carried out using 3,5,3',5'-tetramethylbenzidine (TMB) and o-phenylenediamine (OPD) as the reagents in the presence of H_2O_2 in 0.14 M acetate buffer solution (pH 3.0-8.0). The UV-vis absorbance of the color reaction (at 652 nm for ox TMB and at 445 nm for ox OPD) was recorded at a certain reaction time to express the POD-like activity.

5. Kinetic assay

The steady-state kinetic assay of Mn-N-C NPs with H_2O_2 as the substrate was performed by adding 50 μg/mL Mn-N-C NPs into 0.2 M HAc-NaAc buffer solution (pH 4.0) containing TMB (1 mM) and different concentrations of H_2O_2 (0.125, 0.25, 0.5, 1, 2, 4, 8 mM). The Michaelis constant (K_M) is defined as the substrate concentration at half the maximum reaction rate. K_M reflects the affinity of Mn-N-C NPs for its substrate. Maximal reaction velocity (V_{max}) is the maximal reaction rate that is observed at saturating substrate concentrations. The kinetics constants K_M and V_{max} were calculated through fitting the initial reaction velocity (V) values and the substrate concentrations to equations S3-S5.

$$V=(V_{max}\times[S])/(K_M+[S]) \quad \text{(S3)}$$

Where *[S]* is the concentration of substrate, *V* is the initial velocity and is calculated using the following equation:

$$V=\Delta A/(\Delta t\times\varepsilon\times l) \quad \text{(S4)}$$

where ΔA is the change of absorbance value, Δt is the initial reaction time (s), ε is the molar absorption coefficient of the colorimetric substrate, which is typically 39 000 M^{-1} cm^{-1} at 652 nm for oxidized TMB, and *l* is the path length of light traveling in the cuvette (cm).

The catalytic constant (k_{cat}) is defined as the maximum number of substrate molecules converted to product per unit of time and is calculated by the following equation:

$$k_{cat}=V_{max}/[E] \quad \text{(S5)}$$

where *[E]* is the concentration of Mn-N-C NPs (M).

k_{cat}/K_M characterizes both the affinity and catalytic ability of the enzyme to the substrate, reflecting the catalytic efficiency of Mn-N-C NPs.

6. Superoxide dismutase-like catalytic activity

The superoxide dismutase (SOD)-like catalytic assays were carried out at room temperature by measuring the inhibition of autooxidation of pyrogallol. In detail, chemicals were added into 1 mL of Tris-HCl (0.1 mM, pH 8.2) buffer solution in the following order: 100 μL pyrogallol-HCl (final pyrogallol concentration 0.20 mM, pH 2.0), and (or without) 100 μL materials (final concentration 50 μg/mL) to form a uniform system. The SOD-like activity was assessed by measuring the oxidation peak at 320 nm using a UV-vis spectrophotometer.

7. Catalase-like catalytic activity

The catalase (CAT)-like catalytic assays of materials were carried out by measuring the rate of oxygen production using a SevenExcellenceTM Benchtop Meter. The total volume of the reaction system was 4.5 mL, including H_2O_2 (75 mM), materials (100 μg/mL) and 0.1 M citric acid-Na_2HPO_4 buffer. The pH sensitivity of the catalase-like activity was evidenced by varying the buffer pH from 5.5 to 7.5. The catalase comes from cow liver, 3500 units/mg.

8. Oxidase-like catalytic activity

The OXD-like activity was assessed by adding different time in 0.01 M HAc-NaAc buffer (pH= 5.0), after that 0.1 mM TMB was added and the mixture was incubated for 5 min at 25 °C. The final 652 nm absorbance of mixture was detected by a Bio-Rad 680 microplate reader.

9. GSH consumption

Glutathione (GSH) oxidation was examined by Ellman's assay and all the experiments were carried out in the dark. Ellman reagent 5,5′-dithiobis(2-nitrobenzoic acid) (DTNB) reacted with thiol groups (-SH) in GSH by cleaving its disulfide bonds (-S-S-) to obtain a yellow product 2-nitro-5-thiobenzoate

acid. To confirm the concentration-dependent GSH consumption, Mn-N-C NPs (100, 80, 60, 40, 20 and 0 μg/mL) and H_2O_2 (140 μM) were treated with GSH (225 μL, 0.8 mM) in PBS at 37 °C for 1 h. Similarly, Mn-N-C NPs (100 μL, 0.8 mM) was co-incubated with GSH (225 μL, 0.8 mM) in PBS at varied time (0, 20, 40, 60, 80, 100 and 120 min) to investigate time-dependent GSH consumption. The above solution mixed with DTNB (15 μL, 10 mM). Next, the mixture solution was centrifugated and the supernatant was required for the GSH depletion measurement by UV-Vis absorption spectra. The loss of GSH was calculated as follows:

$$Loss\ of\ GSH\ (\%) = (A_n - A_s)/A_n \times 100 \quad \text{(S6)}$$

where A_s and A_n are the absorbance of the sample and negative control.

10. Antibacterial experiments *in vitro*

The antibacterial ability of Mn-N-C NPs was determined by plate counting method. Briefly, bacteria suspensions (2×10^8 CFU mL^{-1}, 100 μL) were incubated with PBS (control), H_2O_2 (140 μM), $Mn(acac)_3$@ZIF-8 (25 μg mL^{-1}), $Mn(acac)_3$@ZIF-8 (25 μg mL^{-1})+H_2O_2 (140 μM), Mn-N-C NPs (25 μg mL^{-1}), Mn-N-C NPs (25 μg mL^{-1})+H_2O_2 (140 μM) in a 96-well plate, respectively. After incubated at 37 °C for 20 min, the bacteria suspension (diluted by 1-10^4 fold, 100 μL) was spread on the LB agar plates. The number of bacteria colonies was counted and recorded after incubation for 24 h at 37 °C.

11. Protein leakage

MRSA and AREC cells (10^6 CFU/mL) were treated with increasing concentrations of Mn-N-C NPs and 140 μM of H_2O_2 for 1 h at 37 °C and then irradiated for 3 min under 808 nm NIR (1.0 W cm^{-2}). Subsequently, the cells were pelleted down at 5000 rpm for 5 min, and the cell-free supernatant was collected. The concentration of leaked proteins in the supernatant was measured using the standard Bradford assay.

12. Cytoplasmic membrance depolarization

The membrane potential-sensitive fluorescent dye, diSC3(5), was employed as an indicator of membrane depolarization. Overnight cultured bacteria were diluted in a fresh LB broth and cultured to the mid log phase. AREC and MRSA cells were collected by centrifugation and washed with 5 mM PBS and 5 mM glucose. Following that, 1950 μL of the bacterial suspension and 50 μL of 20 μM diSC3(5) were added. The fluorescence of the suspension was monitored at room temperature for 20 min at an excitation wavelength of 622 nm and an emission wavelength of 670 nm. Mn-N-C NPs (0, 20, 30, 40 and 50 μg/mL) and 140 μM of H_2O_2 were added into the cuvette and the increased potential was monitored after irradiated for 3 min under 808 nm NIR (1.0 W cm^{-2}).

13. Biofilm viability

Biofilm formation assays were performed as previously described with some changes. Overnight cultures of MRSA were resuspended in fresh medium (OD_{600} of approximately 0.1). Aliquots of 100 μL of bacterial suspension and final concentrations of 0, 25, 50, 100, 200 and 400 μg/mL of Mn-N-C NPs +H_2O_2 (140 μM) were co-stored in a 96-well plate at 37 °C for 24 h. The medium was removed from the wells and the biofilm was carefully washed twice with PBS to remove planktonic bacteria. The biofilms were fixed with 10% ethanol for 10 min, and then stained with 0.1% crystal violet (CV) for 20 min in each well. After discarding CV, the biofilm samples were washed with PBS, and 33% AcOH was added to dissolve the fuel on the biofilm, then the absorbance at 570 nm was measured using a microplate reader (Tecan Infinite M200 Pro). The percentage viability of the treated biofilm relative to the control was calculated.

14. Bacterial resistance

The strains of MRSA was exposed to sub-MICs of Mn-N-C NPs for sustained passages, and then the MICs of Mn-N-C NPs were determined against each passage of the strain. The freshly diluted MRSA (1.0×10^5 CFU) in the broth medium were cultured in 25 μg/mL Mn-N-C NPs and 140 μM H_2O_2 at 37 °C for 12 h on a shaker bed at 90 rpm, and the sensitivity of each strain passage to Mn-N-C NPs was tested. For comparative analysis, ceftizoxime was used as a control.

15. Cytotoxicity measurement

Cytotoxicity evaluation was performed on Human umbilical vein endothelial cells lines (HUVEC). These cells were implanted into 96-well microplates and permitted to adhere overnight. Subsequently, the culture medium was substituted by fresh culture medium including different samples [PBS, H_2O_2 (5 mM), $Mn(acac)_3$@ZIF-8 (50 μg/mL), $Mn(acac)_3$@ZIF-8 (50 μg/mL)+H_2O_2 (5 mM), Mn-N-C NPs (50 μg/mL) and Mn-N-C NPs (0–200 μg/mL) +H_2O_2 (5 mM)], respectively. After the co-incubation for 24 h, the culture medium was substituted by MTT (20 μg/mL) culture solution and incubation for 4 h. Ultimately, dimethyl sulfoxide (150 μL) was added to each well. Cell viability was calculated by measuring the absorbance at λ = 490 nm to the control via a microplate reader.

16. Hemocompatibility evaluation

Fresh blood from mice was taken and erythrocytes were isolated by centrifugation (1,000 rpm, 10 min). The obtained erythrocytes were washed three times with saline and then diluted to a final concentration of 5% (v/v). The Mn-N-C NPs +H_2O_2 (500 μL) with erythrocyte solution (500 μL) was added into a 24-well microtiter plate and then shaken at 150 rpm for 1 h in an incubator at 37 °C. Afterwards, the microplate contents were centrifuged (1000 rpm, 10 min) and the supernatant (100 μL) was introduced into a 96-well microplate. The absorbance of the solution at 540 nm was determined using a microplate reader (Tecan Infinite M200 Pro). Triton X-100 (0.1%) was used as a positive control. The percentage hemolysis was calculated based on the following relationship:

$$Hemolysis\ percentage\ (\%) = [(A_p\text{-}A_b)/(A_t\text{-}A_b)]\times 100\% \quad (S7)$$

where A_p, A_t, and A_b are the absorbance values of the experimental group, Triton X-100 positive control and saline, respectively.

17. Mice wound model

All animal experiments in this study were approved and compliant with the guidelines of the Institutional Animal Care and Use Committee (IACUC) of Qingdao University of Science and Technology. Male Kunming mice (28–32 g, 5–6 weeks old) were purchased from the Model Animal Research Center (MARC) of Jinan Pengyue Co. Ltd. (JiNan, China). All the mice were divided into seven groups, each group had six mice for conducting parallel experiments. The wound model was built on the back of mice, and each mouse was anaesthetized by isoflurane aerosol and then slashed an 8 mm full-thickness skin wound. MRSA strains (3×10^7 CFU, 50 μL) were injected into each wound for constructing the infected wound model.

After 24 h, the infected mice were anaesthetized again, and then PBS, H_2O_2, Mn-N-C NPs, and Mn-N-C NPs + H_2O_2 were respectively dropwise into the wound for dispersed evenly in each group. After about 10 min, all the mice woke up and moved normally. The above experimental procedures were repeated every day until the fifth day, that was anaesthetizing mice, treating wound with PBS, H_2O_2, Mn-N-C NPs, and Mn-N-C NPs+H_2O_2 respectively. Meanwhile, photographs of the wounds were taken every three days.

For histological analysis, the mice were sacrificed with an overdose of pentobarbital (100 $mg\cdot kg^{-1}$) on day 5. The entire wound with adjacent normal skin was collected and fixed using 4% paraformaldehyde solution for 24 h at 4 °C. The sample of subcutaneous tissue was analyzed using H&E staining method. All sections were observed and photographed with a microscope (BX51, Olympus, Japan), meanwhile, the wound was excised and incubated in sterile saline for 24 h at 37 °C. Then, the culture solution was diluted 100-fold and cultured on LB agar plates at 37 °C for 24 h for counting the number of bacterial colonies. The wound healing rate was calculated as follows:

$$Wound\ healing\ rate\ (\%) = (A_{initial}\text{–}A_{time})/A_{initial}\times 100 \quad (S8)$$

where $A_{initial}$ is the initial wound area (day 0), and A_{time} is the wound area at different time points.

18. Statistical analysis

All data were raw data and expressed as mean ± standard deviation (mean ± SD). The sample size (n) for each statistical analysis was given in each Figure legend. Two-factor ANOVA was used to evaluate the effects of different materials treatments and NIR irradiation on bacterial inhibition rate (Figure 7a, b) or wound healing (Figure 12a, b). The statistical analysis was conducted using Origin 2023b software. Statistical difference was defined as *$p < 0.05$, **$p < 0.01$, ***$p < 0.001$.

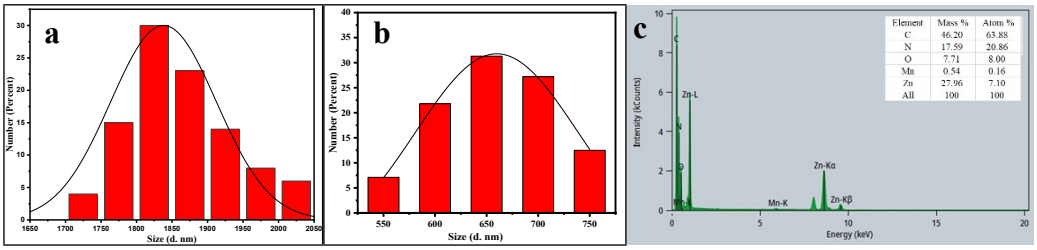

Figure S1. The size distribution histogram of (a) $Mn(acac)_3$@ZIF-8 and (b) Mn-N-C NPs; (c) EDS mapping of Mn-N-C NPs.

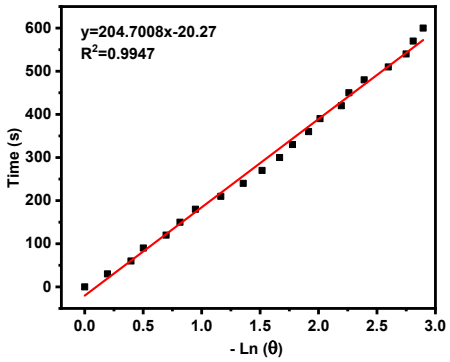

Figure S2. The cooling time plot after 600s vs the negative natural logarithm of driving force temperature (-lnθ) with slope of 204.70 for the concentration of 25 μg mL^{-1}.

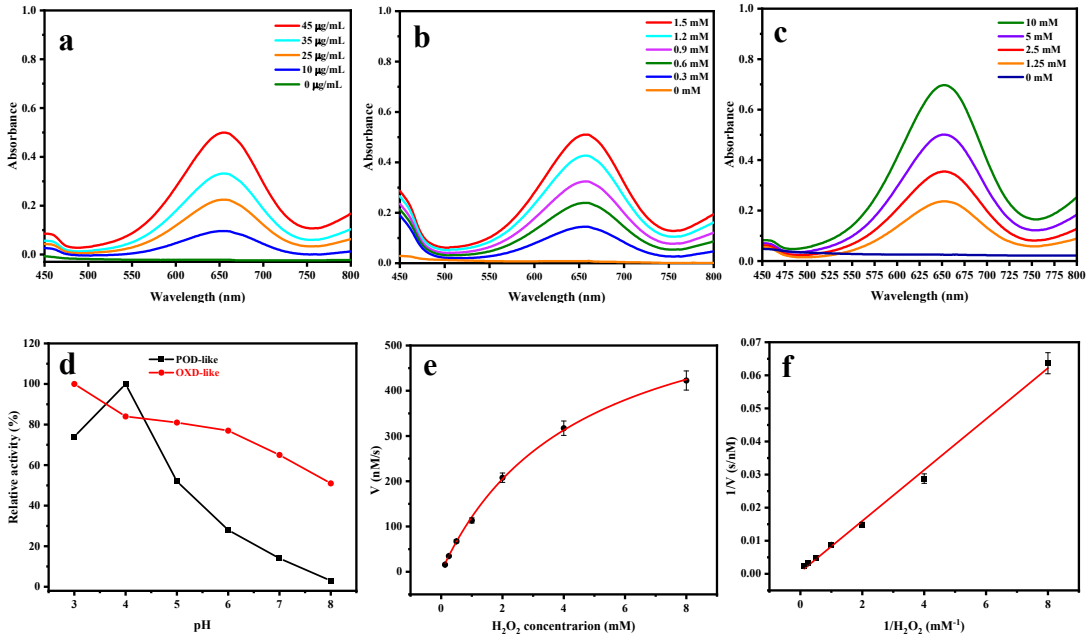

Figure S3. Effect of (a) Mn-N-C NPs concentration, (b) TMB concentration and (c) H_2O_2 concentration on the efficiency of •OH production for TMB+Mn-N-C NPs+H_2O_2; (d) Effect of pH values on the both POD-like and OXD-like catalytic performance; (e) Kinetic assay for the POD-like activity of Mn-N-C NPs with H_2O_2 as substrate; (f) Corresponding double-reciprocal plots of POD-like activity of Mn-N-C NPs at a fixed concentration of TMB (1 mM) versus varying concentration of H_2O_2 (0.125, 0.25, 0.5, 1, 2, 4, 8 mM), data presented as mean ± SD (n = 3).

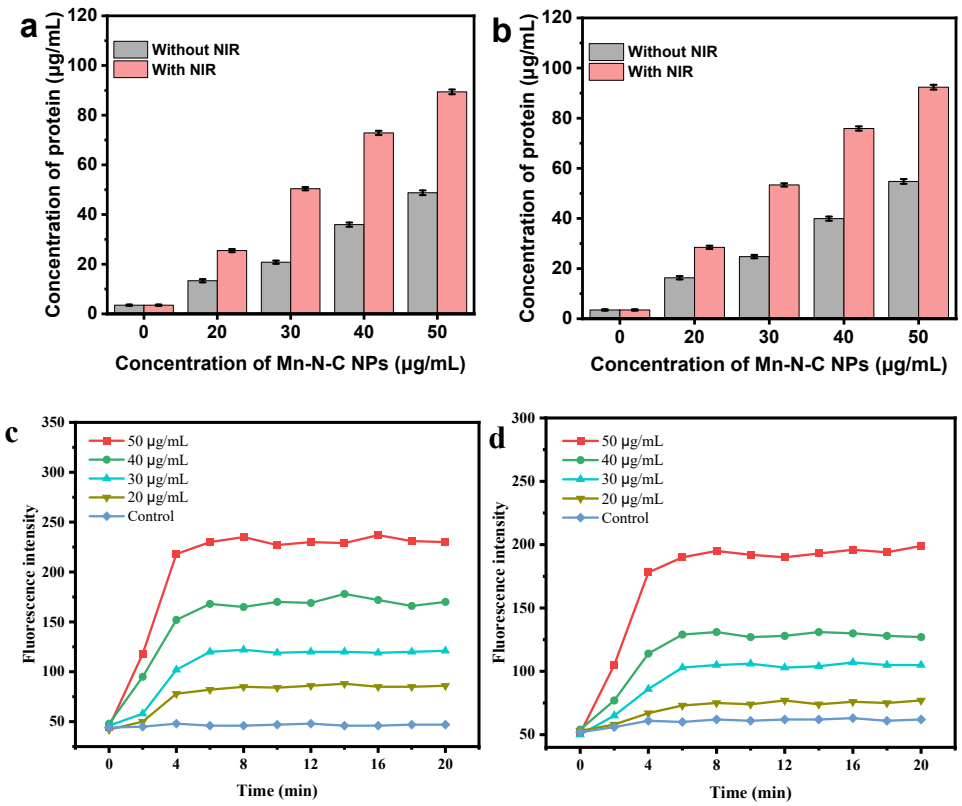

Figure S4. Protein leakage of (a) MRSA and (b) AREC treated with Mn-N-C NPs+ H_2O_2 (NIR, 808 nm, 1.0 W cm^{-2}, 3 min); Membrane depolarization of (c) MRSA and (d) AREC in the presence of Cu_2O-DMB+H_2O_2+NIR (808 nm, 1.0 W cm^{-2}, 3 min).

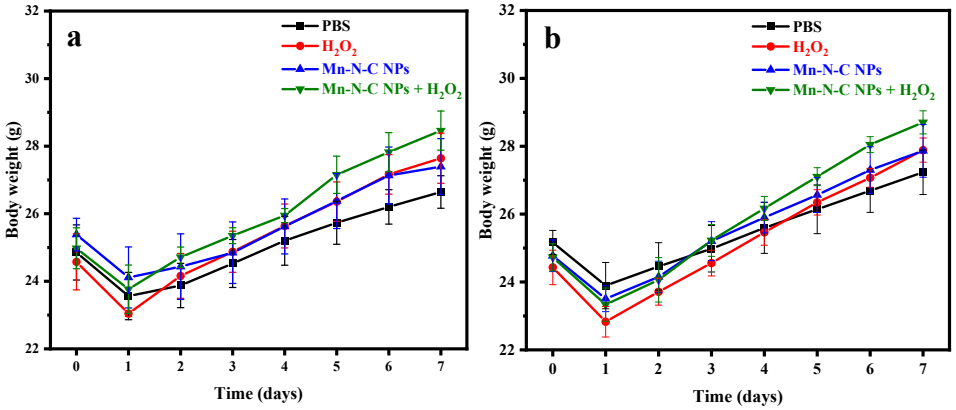

Figure S5. Body weight changes of mice after various treatments (a) without NIR and (b) with NIR (808 nm, 1.0 W cm^{-2}, 3 min). Data presented as mean ± SD (n = 3).

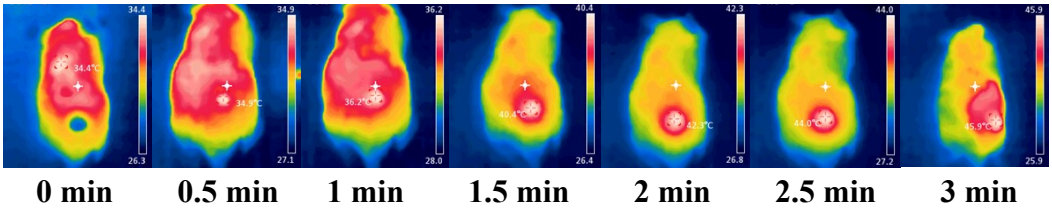

Figure S6. Thermal images of MRSA-infected wounds treated with Mn-N-C NPs+H_2O_2 under NIR laser irradiation (NIR: 808 nm, 1.0 W cm^{-2}, 3 min), ambient temperature is 21.9 ℃, initial body temperature of mice is 34.4 ℃.

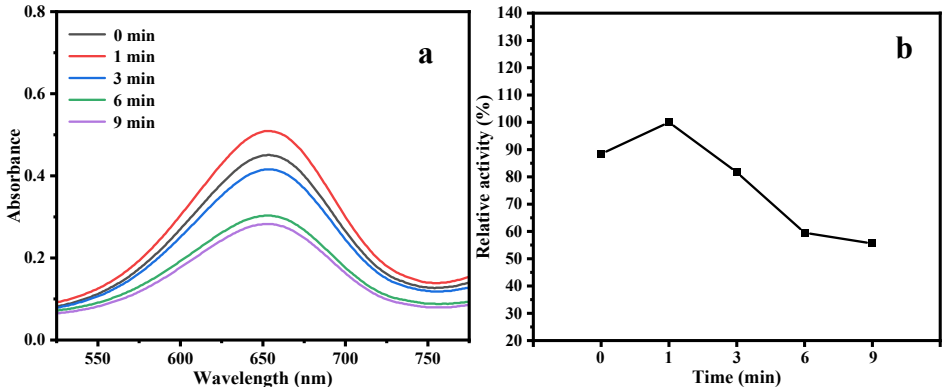

Figure S7. (a) UV-vis absorption spectra of TMB+Mn-N-C NPs+H_2O_2 solution under 808 nm NIR laser irradiation for different times (0 min, 1 min, 3 min, 6 min, 9 min); (b) Effect of 808 nm NIR laser irradiation time on the peroxidase-like catalytic performance;

Table S1. Comparison of Mn-N-C NPs with other similar studies

Name	Mechanism	NIR-photothermal conversion efficiency (η)	The inhibition rate of S.aureus	The inhibition rate of E.coli
CO@mPDA NPs[48]	CO-mediated PTT	26.2%	95.0%	-
PEG-MoS_2 NFs[39]	Unimodal CDT synergized with PTT	43.72%	-	> 99.0%
Mn-N-C NPs (This work)	Multimodal CDT synergized with PTT	40.13%	> 99.0%	> 98.0%